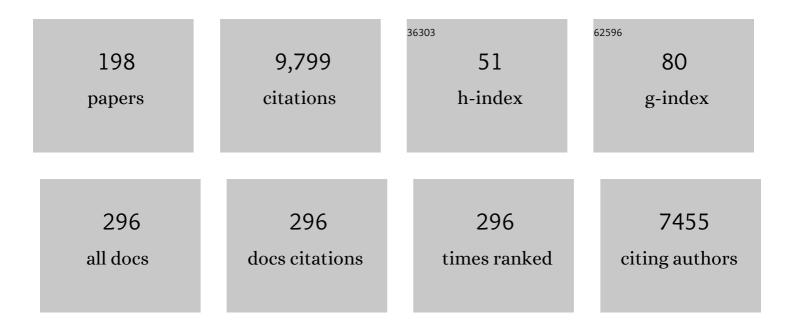
GS Diskin

List of Publications by Year in descending order

Source: https://exaly.com/author-pdf/4127543/publications.pdf Version: 2024-02-01



C S DISKIN

#	Article	IF	CITATIONS
1	Effects of aging on organic aerosol from open biomass burning smoke in aircraft and laboratory studies. Atmospheric Chemistry and Physics, 2011, 11, 12049-12064.	4.9	520
2	Airborne measurement of OH reactivity during INTEX-B. Atmospheric Chemistry and Physics, 2009, 9, 163-173.	4.9	293
3	Evolution of brown carbon in wildfire plumes. Geophysical Research Letters, 2015, 42, 4623-4630.	4.0	284
4	Nitrogen oxides and PAN in plumes from boreal fires during ARCTAS-B and their impact on ozone: an integrated analysis of aircraft and satellite observations. Atmospheric Chemistry and Physics, 2010, 10, 9739-9760.	4.9	234
5	Boreal forest fire emissions in fresh Canadian smoke plumes: C ₁ -C ₁₀ volatile organic compounds (VOCs), CO ₂ , CO, NO ₂ , NO, HCN and	4.9	209
6	Envisions of black carbon, organic, and inorganic aerosols from biomass burning in North America and Asia in 2008. Journal of Geophysical Research, 2011, 116, .	3.3	206
7	C ₂ –C ₁₀ volatile organic compounds (VOCs), CO ₂ , CH ₄ , CO, NO, NO ₂ , NO&:lt:sub&:gt;v&:lt:/sub&:gt:. O&:lt:sub>:3&:lt:/sub>: and	4.9	198
8	Source attribution and interannual variability of Arctic pollution in spring constrained by aircraft (ARCTAS, ARCPAC) and satellite (AIRS) observations of carbon monoxide. Atmospheric Chemistry and Physics, 2010, 10, 977-996.	4.9	189
9	Airborne measurements of western U.S. wildfire emissions: Comparison with prescribed burning and air quality implications. Journal of Geophysical Research D: Atmospheres, 2017, 122, 6108-6129.	3.3	184
10	The Deep Convective Clouds and Chemistry (DC3) Field Campaign. Bulletin of the American Meteorological Society, 2015, 96, 1281-1309.	3.3	165
11	HO _{<i>x</i>} chemistry during INTEXâ€A 2004: Observation, model calculation, and comparison with previous studies. Journal of Geophysical Research, 2008, 113, .	3.3	163
12	On the Sources of Methane to the Los Angeles Atmosphere. Environmental Science & Technology, 2012, 46, 9282-9289.	10.0	126
13	Open-path airborne tunable diode laser hygrometer. , 2002, , .		120
14	Measured and modeled CO and NO y in DISCOVER-AQ: An evaluation of emissions and chemistry over the eastern US. Atmospheric Environment, 2014, 96, 78-87.	4.1	114
15	Ice nucleation and dehydration in the Tropical Tropopause Layer. Proceedings of the National Academy of Sciences of the United States of America, 2013, 110, 2041-2046.	7.1	113
16	Comparison of chemical characteristics of 495 biomass burning plumes intercepted by the NASA DC-8 aircraft during the ARCTAS/CARB-2008 field campaign. Atmospheric Chemistry and Physics, 2011, 11, 13325-13337.	4.9	106
17	Secondary organic aerosol production from local emissions dominates the organic aerosol budget over Seoul, South Korea, during KORUS-AQ. Atmospheric Chemistry and Physics, 2018, 18, 17769-17800.	4.9	105
18	Seasonal variation of the transport of black carbon aerosol from the Asian continent to the Arctic during the ARCTAS aircraft campaign. Journal of Geophysical Research, 2011, 116, .	3.3	104

#	Article	IF	CITATIONS
19	Magnitude and seasonality of wetland methane emissions from the Hudson Bay Lowlands (Canada). Atmospheric Chemistry and Physics, 2011, 11, 3773-3779.	4.9	101
20	Brown carbon aerosol in the North American continental troposphere: sources, abundance, and radiative forcing. Atmospheric Chemistry and Physics, 2015, 15, 7841-7858.	4.9	96
21	Airborne measurements of organosulfates over the continental U.S Journal of Geophysical Research D: Atmospheres, 2015, 120, 2990-3005.	3.3	96
22	Agricultural fires in the southeastern U.S. during SEAC ⁴ RS: Emissions of trace gases and particles and evolution of ozone, reactive nitrogen, and organic aerosol. Journal of Geophysical Research D: Atmospheres, 2016, 121, 7383-7414.	3.3	93
23	TES carbon monoxide validation with DACOM aircraft measurements during INTEXâ€B 2006. Journal of Geophysical Research, 2007, 112, .	3.3	92
24	Cleaner burning aviation fuels can reduce contrail cloudiness. Communications Earth & Environment, 2021, 2, .	6.8	92
25	Characterizing summertime chemical boundary conditions for airmasses entering the US West Coast. Atmospheric Chemistry and Physics, 2011, 11, 1769-1790.	4.9	90
26	Upper tropospheric ozone production from lightning NO <i>_x</i> â€impacted convection: Smoke ingestion case study from the DC3 campaign. Journal of Geophysical Research D: Atmospheres, 2015, 120, 2505-2523.	3.3	88
27	Aerosol optical properties in the southeastern United States in summer – PartÂ1: Hygroscopic growth. Atmospheric Chemistry and Physics, 2016, 16, 4987-5007.	4.9	88
28	Multi-model study of chemical and physical controls on transport of anthropogenic and biomass burning pollution to the Arctic. Atmospheric Chemistry and Physics, 2015, 15, 3575-3603.	4.9	83
29	Racoro Extended-Term Aircraft Observations of Boundary Layer Clouds. Bulletin of the American Meteorological Society, 2012, 93, 861-878.	3.3	81
30	In situ measurements and modeling of reactive trace gases in a small biomass burning plume. Atmospheric Chemistry and Physics, 2016, 16, 3813-3824.	4.9	81
31	Observations of nonmethane organic compounds during ARCTAS â^' Part 1: Biomass burning emissions and plume enhancements. Atmospheric Chemistry and Physics, 2011, 11, 11103-11130.	4.9	80
32	Observations of Saharan dust microphysical and optical properties from the Eastern Atlantic during NAMMA airborne field campaign. Atmospheric Chemistry and Physics, 2011, 11, 723-740.	4.9	80
33	The NASA Airborne Tropical Tropopause Experiment: High-Altitude Aircraft Measurements in the Tropical Western Pacific. Bulletin of the American Meteorological Society, 2017, 98, 129-143.	3.3	79
34	The RELIEF flow tagging technique and its application in engine testing facilities and for helium-air mixing studies. Measurement Science and Technology, 2000, 11, 1272-1281.	2.6	76
35	Observations of total RONO ₂ over the boreal forest: NO _x sinks and HNO ₃ sources. Atmospheric Chemistry and Physics, 2013, 13, 4543-4562.	4.9	76
36	Emission characteristics of black carbon in anthropogenic and biomass burning plumes over California during ARCTAS ARB 2008. Journal of Geophysical Research, 2012, 117, .	3.3	73

#	Article	IF	CITATIONS
37	Revealing important nocturnal and dayâ€toâ€day variations in fire smoke emissions through a multiplatform inversion. Geophysical Research Letters, 2015, 42, 3609-3618.	4.0	73
38	Absorbing aerosol in the troposphere of the Western Arctic during the 2008 ARCTAS/ARCPAC airborne field campaigns. Atmospheric Chemistry and Physics, 2011, 11, 7561-7582.	4.9	70
39	Impact of Bay-Breeze Circulations on Surface Air Quality and Boundary Layer Export. Journal of Applied Meteorology and Climatology, 2014, 53, 1697-1713.	1.5	70
40	Measurement of HO2NO2in the free troposphere during the Intercontinental Chemical Transport Experiment–North America 2004. Journal of Geophysical Research, 2007, 112, .	3.3	68
41	The distribution of sea-salt aerosol in the global troposphere. Atmospheric Chemistry and Physics, 2019, 19, 4093-4104.	4.9	68
42	Source attributions of pollution to the Western Arctic during the NASA ARCTAS field campaign. Atmospheric Chemistry and Physics, 2013, 13, 4707-4721.	4.9	67
43	IASI carbon monoxide validation over the Arctic during POLARCAT spring and summer campaigns. Atmospheric Chemistry and Physics, 2010, 10, 10655-10678.	4.9	65
44	Revisiting the effectiveness of HCHO/NO2 ratios for inferring ozone sensitivity to its precursors using high resolution airborne remote sensing observations in a high ozone episode during the KORUS-AQ campaign. Atmospheric Environment, 2020, 224, 117341.	4.1	65
45	Analysis of satellite-derived Arctic tropospheric BrO columns in conjunction with aircraft measurements during ARCTAS and ARCPAC. Atmospheric Chemistry and Physics, 2012, 12, 1255-1285.	4.9	63
46	Convective transport of water vapor into the lower stratosphere observed during double-tropopause events. Journal of Geophysical Research D: Atmospheres, 2014, 119, 10,941-10,958.	3.3	63
47	Thunderstorms enhance tropospheric ozone by wrapping and shedding stratospheric air. Geophysical Research Letters, 2014, 41, 7785-7790.	4.0	62
48	The POLARCAT Model Intercomparison Project (POLMIP): overview and evaluation with observations. Atmospheric Chemistry and Physics, 2015, 15, 6721-6744.	4.9	62
49	Improved agreement of AIRS tropospheric carbon monoxide products with other EOS sensors using optimal estimation retrievals. Atmospheric Chemistry and Physics, 2010, 10, 9521-9533.	4.9	61
50	The production and persistence of ΣRONO ₂ in the Mexico City plume. Atmospheric Chemistry and Physics, 2010, 10, 7215-7229.	4.9	61
51	Relationships between Ice Water Content and Volume Extinction Coefficient from In Situ Observations for Temperatures from 0° to â^'86°C: Implications for Spaceborne Lidar Retrievals. Journal of Applied Meteorology and Climatology, 2014, 53, 479-505.	1.5	61
52	Secondary organic aerosols from anthropogenic volatile organic compounds contribute substantially to air pollution mortality. Atmospheric Chemistry and Physics, 2021, 21, 11201-11224.	4.9	60
53	Characterization of Upper-Troposphere Water Vapor Measurements during AFWEX Using LASE. Journal of Atmospheric and Oceanic Technology, 2004, 21, 1790-1808.	1.3	59
54	Patterns of CO ₂ and radiocarbon across high northern latitudes during International Polar Year 2008. Journal of Geophysical Research, 2011, 116, .	3.3	59

#	Article	IF	CITATIONS
55	Mapping hydroxyl variability throughout the global remote troposphere via synthesis of airborne and satellite formaldehyde observations. Proceedings of the National Academy of Sciences of the United States of America, 2019, 116, 11171-11180.	7.1	58
56	Supersonic Mass-Flux Measurements via Tunable Diode Laser Absorption and Nonuniform Flow Modeling. AIAA Journal, 2011, 49, 2783-2791.	2.6	56
57	Aerosol transport and wet scavenging in deep convective clouds: A case study and model evaluation using a multiple passive tracer analysis approach. Journal of Geophysical Research D: Atmospheres, 2015, 120, 8448-8468.	3.3	56
58	Lightning NO _{<i>x</i>} Emissions: Reconciling Measured and Modeled Estimates With Updated NO _{<i>x</i>} Chemistry. Geophysical Research Letters, 2017, 44, 9479-9488.	4.0	56
59	Calibration and data retrieval algorithms for the NASA Langley/Ames Diode Laser Hygrometer for the NASA Transport and Chemical Evolution Over the Pacific (TRACE-P) mission. Journal of Geophysical Research, 2003, 108, .	3.3	51
60	Summary of measurement intercomparisons during TRACE-P. Journal of Geophysical Research, 2003, 108, .	3.3	51
61	Aerosol–Cloud–Meteorology Interaction Airborne Field Investigations: Using Lessons Learned from the U.S. West Coast in the Design of ACTIVATE off the U.S. East Coast. Bulletin of the American Meteorological Society, 2019, 100, 1511-1528.	3.3	51
62	Large contribution of biomass burning emissions to ozone throughout the global remote troposphere. Proceedings of the National Academy of Sciences of the United States of America, 2021, 118, .	7.1	51
63	Validating the AIRS Version 5 CO Retrieval With DACOM In Situ Measurements During INTEX-A and -B. IEEE Transactions on Geoscience and Remote Sensing, 2011, 49, 2802-2813.	6.3	50
64	In situ vertical profiles of aerosol extinction, mass, and composition over the southeast United States during SENEX and SEAC ⁴ RS: observations of a modest aerosol enhancement aloft. Atmospheric Chemistry and Physics, 2015, 15, 7085-7102.	4.9	50
65	Frequency and impact of summertime stratospheric intrusions over Maryland during DISCOVERâ€AQ (2011): New evidence from NASA's GEOSâ€5 simulations. Journal of Geophysical Research D: Atmospheres, 2016, 121, 3687-3706.	3.3	49
66	Episodes of cross-polar transport in the Arctic troposphere during July 2008 as seen from models, satellite, and aircraft observations. Atmospheric Chemistry and Physics, 2011, 11, 3631-3651.	4.9	47
67	Evaluation of UT/LS hygrometer accuracy by intercomparison during the NASA MACPEX mission. Journal of Geophysical Research D: Atmospheres, 2014, 119, 1915-1935.	3.3	47
68	Halocarbon Emissions from the United States and Mexico and Their Global Warming Potential. Environmental Science & Technology, 2009, 43, 1055-1060.	10.0	46
69	An aircraftâ€based upper troposphere lower stratosphere O ₃ , CO, and H ₂ O climatology for the Northern Hemisphere. Journal of Geophysical Research, 2010, 115, .	3.3	46
70	Detailed comparisons of airborne formaldehyde measurements with box models during the 2006 INTEX-B and MILAGRO campaigns: potential evidence for significant impacts of unmeasured and multi-generation volatile organic carbon compounds. Atmospheric Chemistry and Physics, 2011, 11, 11867-11894.	4.9	46
71	Impact of largeâ€scale dynamics on the microphysical properties of midlatitude cirrus. Journal of Geophysical Research D: Atmospheres, 2014, 119, 3976-3996.	3.3	46
72	Ozone chemistry in western U.S. wildfire plumes. Science Advances, 2021, 7, eabl3648.	10.3	45

#	Article	IF	CITATIONS
73	Aerosol optical properties in the southeastern United States in summer – PartÂ2: Sensitivity of aerosol optical depth to relative humidity and aerosol parameters. Atmospheric Chemistry and Physics, 2016, 16, 5009-5019.	4.9	44
74	Observing Nitrogen Dioxide Air Pollution Inequality Using High-Spatial-Resolution Remote Sensing Measurements in Houston, Texas. Environmental Science & Technology, 2020, 54, 9882-9895.	10.0	44
75	Investigation of factors controlling PM2.5 variability across the South Korean Peninsula during KORUS-AQ. Elementa, 2020, 8, .	3.2	44
76	Characterization, sources and reactivity of volatile organic compounds (VOCs) in Seoul and surrounding regions during KORUS-AQ. Elementa, 2020, 8, .	3.2	44
77	Tunable infrared laser instruments for airborne atmospheric studies. Applied Physics B: Lasers and Optics, 2008, 92, 409-417.	2.2	42
78	In situ measurements of tropospheric volcanic plumes in Ecuador and Colombia during TC ⁴ . Journal of Geophysical Research, 2011, 116, .	3.3	41
79	Airborne observations of bioaerosol over the Southeast United States using a Wideband Integrated Bioaerosol Sensor. Journal of Geophysical Research D: Atmospheres, 2016, 121, 8506-8524.	3.3	40
80	The impacts of aerosol loading, composition, and water uptake on aerosol extinction variability in the Baltimore–Washington, D.C. region. Atmospheric Chemistry and Physics, 2016, 16, 1003-1015.	4.9	39
81	The NASA Atmospheric Tomography (ATom) Mission: Imaging the Chemistry of the Global Atmosphere. Bulletin of the American Meteorological Society, 2022, 103, E761-E790.	3.3	39
82	Dominant role of mineral dust in cirrus cloud formation revealed by global-scale measurements. Nature Geoscience, 2022, 15, 177-183.	12.9	39
83	An analysis of fast photochemistry over high northern latitudes during spring and summer using in-situ observations from ARCTAS and TOPSE. Atmospheric Chemistry and Physics, 2012, 12, 6799-6825.	4.9	38
84	Large vertical gradient of reactive nitrogen oxides in the boundary layer: Modeling analysis of DISCOVERâ€AQ 2011 observations. Journal of Geophysical Research D: Atmospheres, 2016, 121, 1922-1934.	3.3	38
85	Influence of cloud, fog, and high relative humidity during pollution transport events in South Korea: Aerosol properties and PM2.5 variability. Atmospheric Environment, 2020, 232, 117530.	4.1	37
86	Constraining remote oxidation capacity with ATom observations. Atmospheric Chemistry and Physics, 2020, 20, 7753-7781.	4.9	36
87	Role of convection in redistributing formaldehyde to the upper troposphere over North America and the North Atlantic during the summer 2004 INTEX campaign. Journal of Geophysical Research, 2008, 113, .	3.3	35
88	Reactive nitrogen, ozone and ozone production in the Arctic troposphere and the impact of stratosphere-troposphere exchange. Atmospheric Chemistry and Physics, 2011, 11, 13181-13199.	4.9	35
89	Evaluating high-resolution forecasts of atmospheric CO and CO ₂ from a global prediction system during KORUS-AQ field campaign. Atmospheric Chemistry and Physics, 2018, 18, 11007-11030.	4.9	35
90	Characteristics of the atmospheric CO ₂ signal as observed over the conterminous United States during INTEXâ€NA. Journal of Geophysical Research, 2008, 113, .	3.3	34

#	Article	IF	CITATIONS
91	Pollution transport from North America to Greenland during summer 2008. Atmospheric Chemistry and Physics, 2013, 13, 3825-3848.	4.9	34
92	Correcting model biases of CO in East Asia: impact on oxidant distributions during KORUS-AQ. Atmospheric Chemistry and Physics, 2020, 20, 14617-14647.	4.9	34
93	Nighttime and daytime dark oxidation chemistry in wildfire plumes: an observation and model analysis of FIREX-AQ aircraft data. Atmospheric Chemistry and Physics, 2021, 21, 16293-16317.	4.9	34
94	Impact of the deep convection of isoprene and other reactive trace species on radicals and ozone in the upper troposphere. Atmospheric Chemistry and Physics, 2012, 12, 1135-1150.	4.9	33
95	An elevated reservoir of air pollutants over the Mid-Atlantic States during the 2011 DISCOVER-AQ campaign: Airborne measurements and numerical simulations. Atmospheric Environment, 2014, 85, 18-30.	4.1	33
96	Aircraft-measured indirect cloud effects from biomass burning smoke in the Arctic and subarctic. Atmospheric Chemistry and Physics, 2016, 16, 715-738.	4.9	32
97	Chemical transport models often underestimate inorganic aerosol acidity in remote regions of the atmosphere. Communications Earth & Environment, 2021, 2, .	6.8	32
98	Observation-based modeling of ozone chemistry in the Seoul metropolitan area during the Korea-United States Air Quality Study (KORUS-AQ). Elementa, 2020, 8, .	3.2	32
99	Sources and transport of Δ ¹⁴ C in CO ₂ within the Mexico City Basin and vicinity. Atmospheric Chemistry and Physics, 2009, 9, 4973-4985.	4.9	31
100	Convective distribution of tropospheric ozone and tracers in the Central American ITCZ region: Evidence from observations during TC4. Journal of Geophysical Research, 2010, 115, .	3.3	31
101	Using Shortâ€Term CO/CO ₂ Ratios to Assess Air Mass Differences Over the Korean Peninsula During KORUSâ€AQ. Journal of Geophysical Research D: Atmospheres, 2019, 124, 10951-10972.	3.3	31
102	The Global Budget of Atmospheric Methanol: New Constraints on Secondary, Oceanic, and Terrestrial Sources. Journal of Geophysical Research D: Atmospheres, 2021, 126, e2020JD033439.	3.3	31
103	Convective and wave signatures in ozone profiles over the equatorial Americas: Views from TC4 2007 and SHADOZ. Journal of Geophysical Research, 2010, 115, .	3.3	30
104	Ammonia and methane dairy emission plumes in the San Joaquin Valley of California from individual feedlot to regional scales. Journal of Geophysical Research D: Atmospheres, 2015, 120, 9718-9738.	3.3	30
105	High Temporal Resolution Satellite Observations of Fire Radiative Power Reveal Link Between Fire Behavior and Aerosol and Gas Emissions. Geophysical Research Letters, 2020, 47, e2020GL090707.	4.0	30
106	Steady-state aerosol distributions in the extra-tropical, lower stratosphere and the processes that maintain them. Atmospheric Chemistry and Physics, 2008, 8, 6617-6626.	4.9	29
107	Wet scavenging of soluble gases in DC3 deep convective storms using WRFâ€Chem simulations and aircraft observations. Journal of Geophysical Research D: Atmospheres, 2016, 121, 4233-4257.	3.3	29
108	The NASA Carbon Airborne Flux Experiment (CARAFE): instrumentation and methodology. Atmospheric Measurement Techniques, 2018, 11, 1757-1776.	3.1	29

#	Article	IF	CITATIONS
109	Sea spray aerosol concentration modulated by sea surface temperature. Proceedings of the National Academy of Sciences of the United States of America, 2021, 118, .	7.1	29
110	Impacts of transported background pollutants on summertime western US air quality: model evaluation, sensitivity analysis and data assimilation. Atmospheric Chemistry and Physics, 2013, 13, 359-391.	4.9	28
111	Dehydration in the tropical tropopause layer: A case study for model evaluation using aircraft observations. Journal of Geophysical Research D: Atmospheres, 2014, 119, 5299-5316.	3.3	28
112	On the Susceptibility of Cold Tropical Cirrus to Ice Nuclei Abundance. Journals of the Atmospheric Sciences, 2016, 73, 2445-2464.	1.7	28
113	Rapid cloud removal of dimethyl sulfide oxidation products limits SO ₂ and cloud condensation nuclei production in the marine atmosphere. Proceedings of the National Academy of Sciences of the United States of America, 2021, 118, .	7.1	28
114	Supersonic Coaxial Jet Experiment for Computational Fluid Dynamics Code Validation. AIAA Journal, 2006, 44, 585-592.	2.6	27
115	High Frequency Pulsed Injection into a Supersonic Duct Flow. AIAA Journal, 2013, 51, 809-818.	2.6	27
116	Simulating reactive nitrogen, carbon monoxide, and ozone in California during ARCTAS-CARB 2008 with high wildfire activity. Atmospheric Environment, 2016, 128, 28-44.	4.1	26
117	Anthropogenic emissions during Arctas-A: mean transport characteristics and regional case studies. Atmospheric Chemistry and Physics, 2011, 11, 8677-8701.	4.9	25
118	Airborne quantification of upper tropospheric NO <i>_x</i> production from lightning in deep convective storms over the United States Great Plains. Journal of Geophysical Research D: Atmospheres, 2016, 121, 2002-2028.	3.3	25
119	Missing OH reactivity in the global marine boundary layer. Atmospheric Chemistry and Physics, 2020, 20, 4013-4029.	4.9	25
120	Impacts of the Denver Cyclone on regional air quality and aerosol formation in the Colorado Front Range during FRAPPÉÂ2014. Atmospheric Chemistry and Physics, 2016, 16, 12039-12058.	4.9	24
121	Estimating Source Region Influences on Black Carbon Abundance, Microphysics, and Radiative Effect Observed Over South Korea. Journal of Geophysical Research D: Atmospheres, 2018, 123, 13,527.	3.3	24
122	Formaldehyde evolution in US wildfire plumes during the Fire Influence on Regional to Global Environments and Air Quality experiment (FIREX-AQ). Atmospheric Chemistry and Physics, 2021, 21, 18319-18331.	4.9	24
123	Assimilation of IASI satellite CO fields into a global chemistry transport model for validation against aircraft measurements. Atmospheric Chemistry and Physics, 2012, 12, 4493-4512.	4.9	23
124	Exploring Oxidation in the Remote Free Troposphere: Insights From Atmospheric Tomography (ATom). Journal of Geophysical Research D: Atmospheres, 2020, 125, e2019JD031685.	3.3	23
125	Accumulation-mode aerosol number concentrations in the Arctic during the ARCTAS aircraft campaign: Long-range transport of polluted and clean air from the Asian continent. Journal of Geophysical Research, 2011, 116, .	3.3	22
126	Measurement report: Long-range transport patterns into the tropical northwest Pacific during the CAMP ² Ex aircraft campaign: chemical composition, size distributions, and the impact of convection. Atmospheric Chemistry and Physics, 2021, 21, 3777-3802.	4.9	22

#	Article	IF	CITATIONS
127	Attribution and evolution of ozone from Asian wild fires using satellite and aircraft measurements during the ARCTAS campaign. Atmospheric Chemistry and Physics, 2012, 12, 169-188.	4.9	21
128	In situ measurements of water uptake by black carbonâ€containing aerosol in wildfire plumes. Journal of Geophysical Research D: Atmospheres, 2017, 122, 1086-1097.	3.3	21
129	Source Contributions to Carbon Monoxide Concentrations During KORUSâ€AQ Based on CAMâ€chem Model Applications. Journal of Geophysical Research D: Atmospheres, 2019, 124, 2796-2822.	3.3	21
130	Assessment of Observational Evidence for Direct Convective Hydration of the Lower Stratosphere. Journal of Geophysical Research D: Atmospheres, 2020, 125, e2020JD032793.	3.3	21
131	Airborne formaldehyde and volatile organic compound measurements over the Daesan petrochemical complex on Korea's northwest coast during the Korea-United States Air Quality study. Elementa, 2020, 8, .	3.2	21
132	Characteristics and evolution of brown carbon in western United States wildfires. Atmospheric Chemistry and Physics, 2022, 22, 8009-8036.	4.9	21
133	Ozone profiles in the Baltimore-Washington region (2006–2011): satellite comparisons and DISCOVER-AQ observations. Journal of Atmospheric Chemistry, 2015, 72, 393-422.	3.2	20
134	Physical processes controlling the spatial distributions of relative humidity in the tropical tropopause layer over the Pacific. Journal of Geophysical Research D: Atmospheres, 2017, 122, 6094-6107.	3.3	20
135	Satellite observations of Mexico City pollution outflow from the Tropospheric Emissions Spectrometer (TES). Atmospheric Environment, 2009, 43, 1540-1547.	4.1	19
136	HFC-152a and HFC-134a emission estimates and characterization of CFCs, CFC replacements, and other halogenated solvents measured during the 2008 ARCTAS campaign (CARB phase) over the South Coast Air Basin of California. Atmospheric Chemistry and Physics, 2011, 11, 2655-2669.	4.9	19
137	Scramjet Combustion Efficiency Measurement via Tomographic Absorption Spectroscopy and Particle Image Velocimetry. AIAA Journal, 2016, 54, 2463-2471.	2.6	19
138	Formaldehyde column density measurements as a suitable pathway to estimate nearâ€surface ozone tendencies from space. Journal of Geophysical Research D: Atmospheres, 2016, 121, 13088-13112.	3.3	19
139	Spatial heterogeneity in CO ₂ , CH ₄ , and energy fluxes: insights from airborne eddy covariance measurements over the Mid-Atlantic region. Environmental Research Letters, 2020, 15, 035008.	5.2	19
140	Efficient vibrational Raman conversion in O_2 and N_2 cells by use of superfluorescence seeding. Optics Letters, 1993, 18, 1132.	3.3	18
141	Atmospheric oxidation in the presence of clouds during the Deep Convective Clouds and Chemistry (DC3) study. Atmospheric Chemistry and Physics, 2018, 18, 14493-14510.	4.9	18
142	Understanding and improving model representation of aerosol optical properties for a Chinese haze event measured during KORUS-AQ. Atmospheric Chemistry and Physics, 2020, 20, 6455-6478.	4.9	18
143	Aircraft-based observation of meteoric material in lower-stratospheric aerosol particles between 15 and 68° N. Atmospheric Chemistry and Physics, 2021, 21, 989-1013.	4.9	18
144	Global Atmospheric Budget of Acetone: Airâ€6ea Exchange and the Contribution to Hydroxyl Radicals. Journal of Geophysical Research D: Atmospheres, 2020, 125, e2020JD032553.	3.3	17

#	Article	IF	CITATIONS
145	Evidence of mixing between polluted convective outflow and stratospheric air in the upper troposphere during DC3. Journal of Geophysical Research D: Atmospheres, 2014, 119, 11,477.	3.3	16
146	Saharan dust, convective lofting, aerosol enhancement zones, and potential impacts on ice nucleation in the tropical upper troposphere. Journal of Geophysical Research D: Atmospheres, 2017, 122, 8833-8851.	3.3	16
147	Heterogeneous Ice Nucleation in the Tropical Tropopause Layer. Journal of Geophysical Research D: Atmospheres, 2018, 123, 12,210.	3.3	16
148	Assessing Measurements of Pollution in the Troposphere (MOPITT) carbon monoxide retrievals over urban versus non-urban regions. Atmospheric Measurement Techniques, 2020, 13, 1337-1356.	3.1	16
149	Airborne Measurements of Contrail Ice Properties—Dependence on Temperature and Humidity. Geophysical Research Letters, 2021, 48, e2020GL092166.	4.0	16
150	Chemical Tomography in a Fresh Wildland Fire Plume: A Large Eddy Simulation (LES) Study. Journal of Geophysical Research D: Atmospheres, 2021, 126, e2021JD035203.	3.3	16
151	Intercomparison and evaluation of satellite peroxyacetyl nitrate observations in the upper troposphere–lower stratosphere. Atmospheric Chemistry and Physics, 2016, 16, 13541-13559.	4.9	15
152	Ambient aerosol properties in the remote atmosphere from global-scale in situ measurements. Atmospheric Chemistry and Physics, 2021, 21, 15023-15063.	4.9	15
153	Airborne Emission Rate Measurements Validate Remote Sensing Observations and Emission Inventories of Western U.S. Wildfires. Environmental Science & amp; Technology, 2022, 56, 7564-7577.	10.0	15
154	Meteorological and air quality forecasting using the WRF–STEM model during the 2008 ARCTAS field campaign. Atmospheric Environment, 2011, 45, 6901-6910.	4.1	14
155	Large biogenic contribution to boundary layer O ₃ O regression slope in summer. Geophysical Research Letters, 2017, 44, 7061-7068.	4.0	14
156	Characterizing CO and NO _{<i>y</i>} Sources and Relative Ambient Ratios in the Baltimore Area Using Ambient Measurements and Source Attribution Modeling. Journal of Geophysical Research D: Atmospheres, 2018, 123, 3304-3320.	3.3	14
157	The MOPITT Version 9 CO product: sampling enhancements and validation. Atmospheric Measurement Techniques, 2022, 15, 2325-2344.	3.1	14
158	Measurements on NASA Langley Durable Combustor Rig by TDLAT: Preliminary Results. , 2013, , .		13
159	Two-dimensional imaging of molecular hydrogen in H_2–air diffusion flames using two-photon laser-induced fluorescence. Optics Letters, 1991, 16, 660.	3.3	12
160	Fundamental Mixing and Combustion Experiments for Propelled Hypersonic Flight. , 2002, , .		12
161	Summary of the High Ice Water Content (HIWC) RADAR Flight Campaigns. , 0, , .		12
162	Spatial and temporal variability of trace gas columns derived from WRF/Chem regional model output: Planning for geostationary observations of atmospheric composition. Atmospheric Environment, 2015, 118, 28-44.	4.1	11

#	Article	IF	CITATIONS
163	Direct Measurement of Combustion Efficiency of a Dual-Mode Scramjet via TDLAT and SPIV (Invited). , 2015, , .		11
164	Estimator of Surface Ozone Using Formaldehyde and Carbon Monoxide Concentrations Over the Eastern United States in Summer. Journal of Geophysical Research D: Atmospheres, 2018, 123, 7642-7655.	3.3	11
165	Novel Analysis to Quantify Plume Crosswind Heterogeneity Applied to Biomass Burning Smoke. Environmental Science & Technology, 2021, 55, 15646-15657.	10.0	11
166	Conventional/laser diagnostics to assess flow quality in a combustion-heated facility. , 1999, , .		10
167	High frequency supersonic pulsed injection. , 2001, , .		10
168	Modeling Regional Pollution Transport Events During KORUSâ€AQ: Progress and Challenges in Improving Representation of Landâ€Atmosphere Feedbacks. Journal of Geophysical Research D: Atmospheres, 2018, 123, 10732-10756.	3.3	10
169	Evaluation of Secondary Organic Aerosol (SOA) Simulations for Seoul, Korea. Journal of Advances in Modeling Earth Systems, 2022, 14, .	3.8	10
170	Reconciling Assumptions in Bottomâ€Up and Topâ€Down Approaches for Estimating Aerosol Emission Rates From Wildland Fires Using Observations From FIREXâ€AQ. Journal of Geophysical Research D: Atmospheres, 2021, 126, .	3.3	10
171	Variability of O3 and NO2 profile shapes during DISCOVER-AQ: Implications for satellite observations and comparisons to model-simulated profiles. Atmospheric Environment, 2016, 147, 133-156.	4.1	9
172	Evaluation of deep convective transport in storms from different convective regimes during the DC3 field campaign using WRFâ€Chem with lightning data assimilation. Journal of Geophysical Research D: Atmospheres, 2017, 122, 7140-7163.	3.3	9
173	UAS Chromatograph for Atmospheric Trace Species (UCATS) – a versatile instrument for trace gas measurements on airborne platforms. Atmospheric Measurement Techniques, 2021, 14, 6795-6819.	3.1	9
174	Cold Air Outbreaks Promote New Particle Formation Off the U.S. East Coast. Geophysical Research Letters, 2022, 49, .	4.0	9
175	Photochemical evolution of the 2013 California Rim Fire: synergistic impacts of reactive hydrocarbons and enhanced oxidants. Atmospheric Chemistry and Physics, 2022, 22, 4253-4275.	4.9	9
176	Observation of vibrational relaxation dynamics in X3Sigma(-)g oxygen following stimulated Raman excitation to the $v=1$ level - Implications for the RELIEF flow tagging technique. , 1996, , .		8
177	Implementation of Maximum-Likelihood Expectation-Maximization Algorithm for Tomographic Reconstruction of TDLAT Measurements. , 2014, , .		8
178	Large hemispheric difference in nucleation mode aerosol concentrations in the lowermost stratosphere at mid- and high latitudes. Atmospheric Chemistry and Physics, 2021, 21, 9065-9088.	4.9	8
179	Seasonal Variability in Local Carbon Dioxide Biomass Burning Sources Over Central and Eastern US Using Airborne In Situ Enhancement Ratios. Journal of Geophysical Research D: Atmospheres, 2021, 126, e2020JD034525.	3.3	8
180	Effect of local and regional sources on the isotopic composition of nitrous oxide in the tropical free troposphere and tropopause layer. Journal of Geophysical Research, 2010, 115, .	3.3	7

#	Article	IF	CITATIONS
181	Characteristics of greenhouse gas concentrations derived from ground-based FTS spectra at Anmyeondo, South Korea. Atmospheric Measurement Techniques, 2018, 11, 2361-2374.	3.1	7
182	Spatially Resolved Temperature and Water Vapor Concentration Distributions in a Flat Flame Burner by Tunable Diode Laser Absorption Tomography. , 2011, , .		6
183	Evolution of formaldehyde (HCHO) in a plume originating from a petrochemical industry and its volatile organic compounds (VOCs) emission rate estimation. Elementa, 2021, 9, .	3.2	6
184	Observations of atmospheric oxidation and ozone production in South Korea. Atmospheric Environment, 2022, 269, 118854.	4.1	6
185	Comparison of Water Vapor Measurements by Airborne Sun Photometer and Diode Laser Hygrometer on the NASA DC-8. Journal of Atmospheric and Oceanic Technology, 2008, 25, 1733-1743.	1.3	5
186	Vertical Transport, Entrainment, and Scavenging Processes Affecting Trace Gases in a Modeled and Observed SEAC 4 RS Case Study. Journal of Geophysical Research D: Atmospheres, 2020, 125, e2019JD031957.	3.3	5
187	Field observational constraints on the controllers in glyoxal (CHOCHO) reactive uptake to aerosol. Atmospheric Chemistry and Physics, 2022, 22, 805-821.	4.9	5
188	Polarimeter + Lidar–Derived Aerosol Particle Number Concentration. Frontiers in Remote Sensing, 2022, 3, .	3.5	5
189	An Evaluation of the Representation of Tropical Tropopause Cirrus in the CESM/CARMA Model Using Satellite and Aircraft Observations. Journal of Geophysical Research D: Atmospheres, 2019, 124, 8659-8687.	3.3	4
190	Observations and hypotheses related to low to middle free tropospheric aerosol, water vapor and altocumulus cloud layers within convective weather regimes: a SEAC ⁴ RS case study. Atmospheric Chemistry and Physics, 2019, 19, 11413-11442.	4.9	4
191	Wintertime Nitrous Oxide Emissions in the San Joaquin Valley of California Estimated from Aircraft Observations. Environmental Science & Technology, 2021, 55, 4462-4473.	10.0	4
192	Heterogeneity and chemical reactivity of the remote troposphere defined by aircraft measurements. Atmospheric Chemistry and Physics, 2021, 21, 13729-13746.	4.9	4
193	Correction to "An aircraft-based upper troposphere lower stratosphere O3, CO, and H2O climatology for the Northern Hemisphereâ€: Journal of Geophysical Research, 2010, 115, .	3.3	3
194	Chemical composition of tropospheric air masses encountered during high altitude flights (>11.5Åkm) during the 2009 fall Operation Ice Bridge field campaign. Journal of Geophysical Research, 2012, 117, .	3.3	3
195	Validation of XCO ₂ and XCH ₄ retrieved from a portable Fourier transform spectrometer with those from in situ profiles from aircraft-borne instruments. Atmospheric Measurement Techniques, 2020, 13, 5149-5163.	3.1	3
196	Relationships between supermicrometer particle concentrations and cloud water sea salt and dust concentrations: analysis of MONARC and ACTIVATE data. Environmental Science Atmospheres, 2022, 2, 738-752.	2.4	3
197	Corrigendum to "In situ vertical profiles of aerosol extinction, mass, and composition over the southeast United States during SENEX and SEAC ⁴ RS: observations of a modest aerosol enhancement aloft" published in Atmos. Chem. Phys., 15, 7085–7102, 2015. Atmospheric Chemistry and Physics. 2015. 15, 8455-8455.	4.9	1

198 Diode laser analysis of the sealed enclosures of the Charters of Freedom. , 2002, , .

0